

#### **PAPER**

# Advanced picosecond precision Radio Frequency Timer

To cite this article: S. Zhamkochyan et al 2024 JINST 19 C02014

View the <u>article online</u> for updates and enhancements.





RECEIVED: December 11, 2023 Accepted: January 2, 2024 Published: February 2, 2024

16<sup>TH</sup> Topical Seminar on Innovative Particle and Radiation Detectors Siena, Italy 22–29 September 2023

# **Advanced picosecond precision Radio Frequency Timer**

- S. Zhamkochyan, <sup>a</sup> V. Kakoyan, <sup>a</sup>, <sup>a</sup> S. Abrahamyan, <sup>a</sup> H. Elbakyan, <sup>a</sup> G. Ayvazyan, <sup>a</sup> R. Ayvazyan, <sup>a</sup> A. Ghalumyan, <sup>a</sup> A. Kakoyan, <sup>a</sup> S. Mayilyan, <sup>a</sup> A. Papyan, <sup>a</sup> A. Piloyan, <sup>a</sup> H. Rostomyan, <sup>a</sup> A. Safaryan, <sup>a</sup> G. Sughyan, <sup>a</sup> H. Vardanyan, <sup>a</sup> H. Zohrabyan, <sup>a</sup> J. Annand, <sup>b</sup> K. Livingston, <sup>b</sup> R. Montgomery, <sup>b</sup> P. Achenbach, <sup>c</sup> J. Pochodzalla, <sup>d</sup> D.L. Balabanski, <sup>e</sup>
- S.N. Nakamura, f A. Aprahamian, g M. Brodeur, g V. Sharyy, h D. Yvon h and A. Margaryan h

E-mail: kakoyan@yerphi.am

ABSTRACT: A new type of radio frequency (RF) timing technique is presented. It is based on a helical deflector, which performs circular or elliptical sweeps of photo- or secondary electrons, accelerated to keV energies, by means of RF fields in the 500–1000 MHz range. By converting a time distribution of the electrons to a hit position distribution on a circle or ellipse, this device achieves extremely precise timing, similar to streak cameras. Detection of the scanned electrons, using a position sensitive detector based on microchannel plates and a delay line anode, resulted in a timing resolution of 10 ps, which can be potentially improved to 1 ps. RF-Timer-based single photon and heavy ion detectors have potential applications in different fields of science and industry, which include high energy nuclear physics and imaging technologies. This technique could play a crucial role in developing of sub 10 ps Time-of-Flight Positron Emission Tomography.

Keywords	: Timing	detectors;	Heavy-ion	detectors;	Photon	detectors	for UV,	visible and	IR phot	ons
(vacuum)										

<sup>&</sup>lt;sup>a</sup>A.I. Alikhanyan National Science Laboratory (Yerevan Physics Institute),

<sup>2</sup> Alikhanyan Brothers, Yerevan, Armenia

<sup>&</sup>lt;sup>b</sup>School of Physics & Astronomy, University of Glasgow, University Avenue, Glasgow, U.K.

<sup>&</sup>lt;sup>c</sup>Jefferson Laboratory, 12000 Jefferson Avenue, Newport News, VA, U.S.A.

<sup>&</sup>lt;sup>d</sup>Institute of Nuclear Physics, Johannes Gutenberg University Mainz, Saarstraße 21, Mainz, Germany

<sup>&</sup>lt;sup>e</sup>Extreme Light Infrastructure-Nuclear Physics (ELI-NP), Reactorului Street, Magurele, Romania

<sup>&</sup>lt;sup>f</sup>Department of Physics, the University of Tokyo, 7-3-1 Hongo, Bunkyo-ku, Tokyo, Japan

<sup>&</sup>lt;sup>g</sup> Department of Physics and Astronomy, University of Notre Dame, Holy Cross Dr, Notre Dame, IN, U.S.A.

<sup>&</sup>lt;sup>h</sup>The Particle Physics Division, Saclay, 3 rue Joliot Curie Bâtiment Breguet, Gif-sur-Yvette, France

<sup>\*</sup>Corresponding author.

1	Introduction	1
2	The RF Timer	1
3	RFT and RFPMT: applications in nuclear physics	4
4	RFPMT: applications in imaging technologies	5
	4.1 Time-of-Flight Positron-Emission-Tomography	5
	4.2 Time-of-Flight Diffuse-Optical-Tomography	6
5	Summary	7

## 1 Introduction

**Contents** 

High precision measurement of time is essential in many fields of science and technology. The recently developed timing processor, the Radio Frequency Timer (RFT) [1], and RFT developments such as a photon sensor (the Radio Frequency Photo-Multiplier Tube, RFPMT) and a Fission Fragment Detector (FFD), can achieve ps resolution for single particle detection at MHz rates. They have potential applications in different fields of science and industry, which include high energy nuclear physics and imaging technologies [1, 2].

At present, the detection of optical signals, down to the single-photon level, may be carried out with Avalanche Photodiodes (APD), vacuum Photomultiplier Tubes (PMT), Hybrid Photon Detectors (HPD) and Superconducting Nanowire Single-Photon Detectors (SNSPD). The time resolution limit of current APD, PMT or HPD for single photon detection is about 100 ps full width at half maximum (FWHM), while SNSPD devices have recently reached below 5 ps [3]. The dead time of these devices is typically a few tens of ns. By comparison the RFT, after some optimization and with a multi pixel anode, will offer around 1 ps resolution and a dead time of a few ps. With fast readout from an appropriate pixelated anode, the RFPMT could achieve 100 MHz and higher detection rates.

# 2 The RF Timer

The experimental test setup of the RF Timer is schematically shown in figure 1. It consists of an RF synchronized light source, a photocathode, an accelerating electrode, a permanent magnet, an electrostatic lens, an RF deflector, a Microchannel Plate (MCP) based position sensitive single electron detector (PSD), pulse processing electronics, an RF generator, a data acquisition system and a vacuum system. The RF Timer is operated in a vacuum under  $10^{-6}$  Torr.

UV photons (3) from a diode or pulsed laser enter the tube through a quartz window (2) after deflection from a mirror (1) and are incident on a tantalum photocathode (8). Photoelectrons (PE) produced in the cathode are accelerated by a voltage  $V \sim 2.5\,\text{kV}$  applied between the cathode and an accelerating electrode (7) and then deflected through 90 deg. by a permanent magnet (4). They

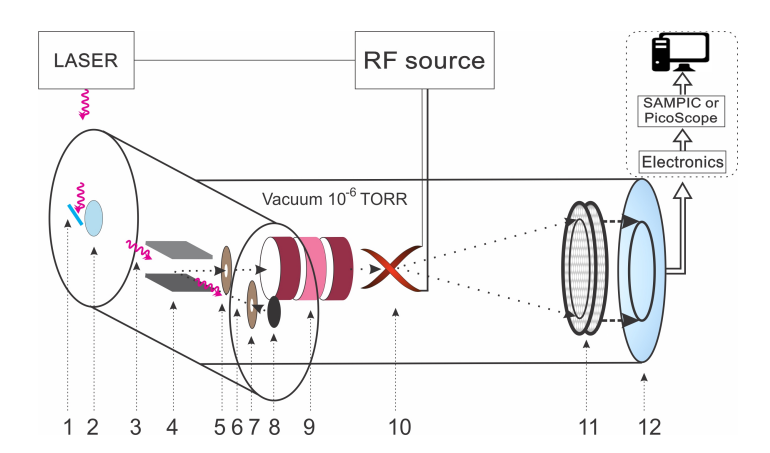


**Figure 1.** Schematic of the RF Timer test setup. 1 – mirror; 2 – quartz window; 3 – photons; 4 – magnet; 5 – collimator; 6 – photoelectron; 7 – accelerating electrode; 8 – photocathode; 9 – electrostatic lens; 10 – RF deflector; 11 – MCPs; 12 – delay line anode.

pass through a collimator (5) and enter into an electrostatic lens (9), which focuses the electrons on to the center of the PSD. This consisted of an MCP system, where the electrons are multiplied by a factor of  $10^6$ , (11) and a DLD40 [4] delay-line (DL) anode (12), producing position-sensitive signals with rise times of a few ns. On their way to the PSD, the electrons pass through a helical RF deflector (10) based on half period helical electrodes and a 500–1000 MHz RF source [5]. Pulses are analyzed by the data acquisition system consisting of a digital scope (such as SAMPIC [6] or Picoscope [7]) and a PC. In this configuration the RFT effectively operates as a Radio Frequency Photomultiplier Tube (RFPMT) [8], capable of timing the arrival of single photons.

The timing resolution of the prototype RFPMT has been measured at the CANDLE, AREAL laser facility [9] which provided 258 nm (4.8 eV) photon bunches (0.45 ps FWHM) phase locked to a 500 MHz oscillator, at a repetition rate of 100 Hz. These bunches were directed to the tantalum disc cathode and the 500 MHz AREAL master oscillator was used to power the RF deflector and therefore provided a time reference. Electrons, produced by the incident photon pulses of the laser, are circularly scanned on to the DL anode, giving X and Y coordinates. A transform to polar coordinates yields the radius R and phase  $\varphi$ , which is proportional to time (the  $2\pi$  period corresponds to 1/500 MHz = 2 ns). As the laser pulse length is short, all photoelectrons effectively have the same phase and a spot on the scanning circle is obtained. The spread in phase of these points represents the overall time resolution of the system, which includes factors related to the laser, the laser and RF oscillator synchronization device and the intrinsic time resolution of the RFPMT.

Results with four different fixed phases are displayed in figure 2, where the equivalent time difference between these phases is about 100 ps. The point in the center of figure 2 (left) is a 2D image of the 2.5 keV electrons, obtained when the RF is OFF. The circle is an image of the scanned electrons, when the 500 MHz RF is ON, but not synchronized with the laser and the color spots on the circle correspond to phase distributions of RF-synchronized photoelectrons for the four different fixed phases. The 1D distributions of these phases are shown in figure 2 (middle) and demonstrate that the time resolution is  $\sim 10 \text{ ps}$ .

An analysis of the various factors which contribute to the time resolution of the RFPMT has identified chromatic aberration, due to the emitted PE's initial energy spread  $\Delta\varepsilon$ , as the largest contributor. The electrons' transit time spread for  $\Delta\varepsilon = 0.7$  eV, simulated using the SIMION software package

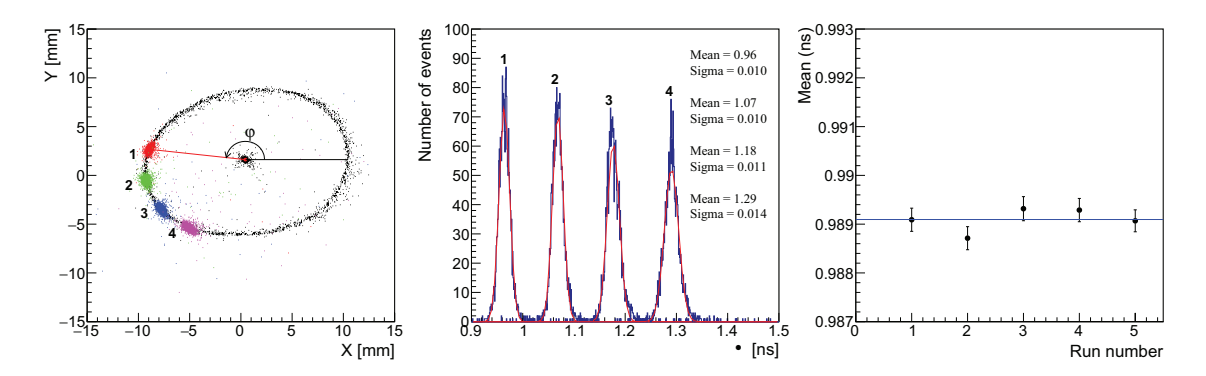


**Figure 2.** Left: 2D images of anode hit positions. Middle: distributions of phases. Right: timing stability measurement.

amounts to  $\sim$ 8 ps. The other significant contribution comes from the intrinsic size of the electron beam spot (or the position resolution of the DL anode), which, taking into account the RF period and the radius of the scanned circle, results in  $\sim$ 6.5 ps uncertainty. In quadrature, these contributions amount to 10.3 ps, which is in good agreement with the results shown in figure 2 (middle). The simulations also show, that after some optimizations, the time resolution of the RFPMT can be improved to 1 ps or better.

The time stability was investigated in a series of measurements at a fixed phase, carried out at  $\sim 10$  min intervals. The mean values of the sequentially measured phase distributions are shown in figure 2 (right), demonstrating that the time stability of the RF PMT over a period of  $\sim 1$  hour is about 0.5 ps, FWHM.

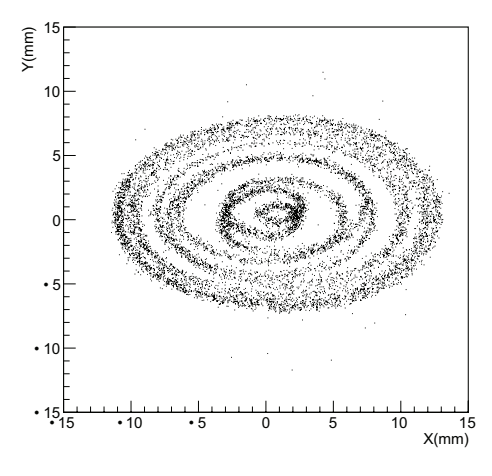


Figure 3. Scanned thermo-electrons image from the RF Timer with two frequencies: 500 MHz and 550 MHz.

At 500 MHz RF frequency the period of pico-time measurement (the dynamic range) is 2 ns. This period can be extended by using 2 helical deflectors or one deflector, powered at two slightly different frequencies. The beat in amplitude from the superimposed frequencies results in "spiral scanning" and offers periods of some tens of ns [10]. Preliminary studies were carried out using a test setup similar to the one described above, with a continuous beam of thermo-electrons emitted from the tantalum disc cathode. The image resulting from scanning the thermo-electrons at two frequencies, 500 MHz and 550 MHz, is shown in figure 3. Those two frequencies come from the same 50 MHz master oscillator as its 10th and 11th multiples.

However more complicated scanning patterns require a more sophisticated PSD and developments employing TimePix4 [11] are being investigated.

# 3 RFT and RFPMT: applications in nuclear physics

High precision measurements of the binding energies of light hypernuclei, with an uncertainty of ~0.01 MeV, are needed to discriminate between various theoretical models [12–14]. In 2007 the use of magnetic spectrometers to precisely measure the momenta of pions from weak two-body decays of electroproduced hyperfragments was proposed for Jefferson Lab [15, 16]. A similar experimental program was started at the electron microtron in Mainz (MAMI) [17–20], where the first high resolution pion spectroscopy from decays of strange systems was performed by electron scattering off a <sup>9</sup>Be target [18–20]. The pion momentum distribution shows a monochromatic peak at p ≈ 133 MeV/c, corresponding to the unique signature for the two-body decay of hyper hydrogen  $^4_{\Lambda} H \rightarrow ^4 He + \pi^-$ , where the  $^4_{\Lambda} H$  stopped inside the target. Its binding energy was determined to be  $2.12\pm0.01(\text{stat.})\pm0.09(\text{sys.})$  MeV with respect to the  $^3\text{H} + \Lambda$  mass. The systematic error was attributed to the uncertainty in the absolute calibration of the magnetic spectrometer. Recently, we proposed a new method for absolute momentum calibration of magnetic spectrometers used in nuclear physics, using the Time-of-Flight (TOF) differences of pairs of particles with different masses. A Cherenkov detector, read out by a RFPMT, was considered as the high-resolution and highly stable TOF detector. By means of Monte Carlo simulations it was demonstrated that the magnetic spectrometers at the MAMI electron-scattering facility can be calibrated absolutely with an accuracy  $\delta p/p \le 10^{-4}$ , which will be crucial for high precision determination of binding energies of the  $\Lambda$  particle in the nuclear ground state [21].

The RFPMT based Cherenkov detectors, with ~10 ps time resolution, allow the realization of a new type nuclear spectroscopy, "delayed-pion" spectroscopy [22] at modern electron accelerators. This will increase the decay pion statistics by about two orders of magnitude compared to experiments proposed at Jefferson Lab or carried out at MAMI. In addition, by measuring lifetimes of the low-lying states and by applying the "tagged-weak  $\pi$ -method" [23], electromagnetic rates of hypernuclear states with lifetimes down to  $10^{-11}$  s could be investigated. This is a further new avenue for hypernuclear studies at RF driven electron, photon and proton beams.

The strength of weak interactions can be determined by precisely measuring the lifetimes of  $\Lambda$ -hypernuclei. The  $\Lambda$  hypernuclear lifetime is expected to reach a constant value (saturation) when medium to heavy hypernuclear masses are reached [24–27]. The dominant two-body channels for this decay include both proton ( $\Lambda p \rightarrow np$ ) and neutron stimulated ( $\Lambda n \rightarrow nn$ ) weak interactions, but there are also a smaller contributions from the three body channel, i.e.  $\Lambda NN \rightarrow nNN(+176 \, \text{MeV})$ , in which the  $\Lambda$  particle interacts with a correlated nucleon pair. One would also expect that there is a limit on the nucleon pairs accessible by the  $\Lambda$  particle due to its limited interaction range. Therefore, the lifetime is expected to "saturate" in heavier hypernuclei. The two most recent theory calculations [26, 27] predict the saturation at around 190 ps and 220 ps respectively. However, it has been difficult to verify this behavior in experimental studies ([28] and refences therein). A measurement of the lifetime to a precision of a few percent will guide and constrain the theoretical input, leading to a more precise determination of the hyperon-nucleon weak interaction.

Fission isomers or shape isomers are nuclear isomers with strongly suppressed de-excitation to the ground state. In general, these states either de-excite to the ground state far more slowly than a "usual"

excited state, or they undergo spontaneous fission with a half-life in the range from few picoseconds to milliseconds. The study of these isomers offers the unique possibility to test our current understanding of nuclear structure at very large deformation. The current knowledge of lifetimes of fission isomers are very limited in the sub nanosecond region. Out of more than 40 fission isomers only a few are known in the picosecond range ([29] and references therein). Most of such measurements were performed via indirect time measurement. New precise direct measurement of lifetimes in the ps-ns region may provide currently missing data for testing existing theory and developing new nuclear models.

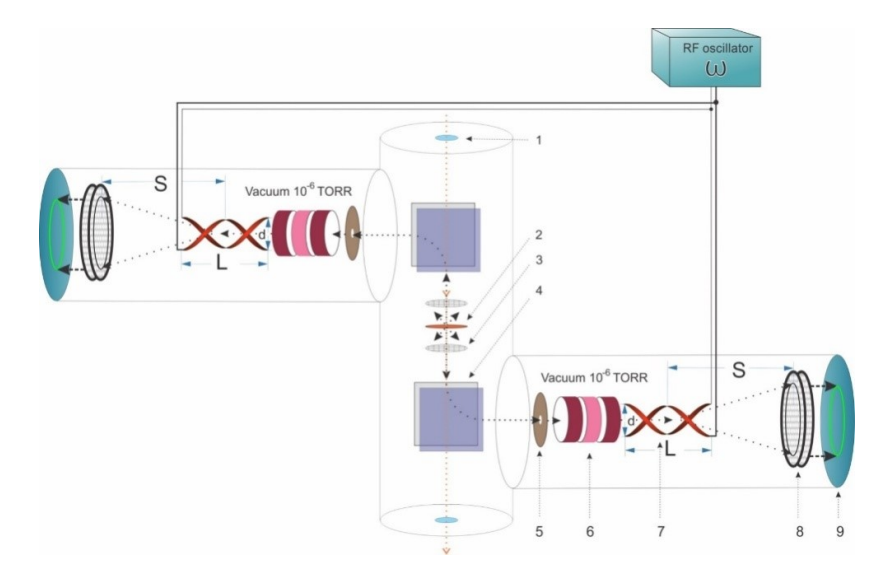


**Figure 4.** Schematic of RF FFD. 1 - beam window; 2 - target, 3 - accelerating electrode, 4 - magnet, 5 - collimator, 6 - electrostatic lens, 7 - RF deflector, 8 - MCP based PSD, 9 - readout electronics.

The RF Timer based Fission Fragment Detector (RF FFD) has been developed, built and is currently being tested. The principle of operation of the RF FFD is schematically shown in figure 4. The primary, RF driven short bunches of electrons, photons or protons hit the target and produce secondary electrons (SE) and reaction products, e.g., prompt, or delayed fission fragments (FF). The FF exiting from the target also produce a few tens of SEs. These electrons are registered by means of the RF Timer. The detection of the fragments in the detectors' two symmetrical arms with  $\sim 10$  ps time coincidence resolution will minimize the possible events from background processes and dark noise in the MCP detectors. The high time resolution of RF FFD ( $\sim 10$  ps) allows separation of prompt and delayed events. This detector would be, in particular, very well suited for direct precise measurements of the hypernuclear and fission isomers lifetimes at RF driven electron, photon and proton beams.

# 4 RFPMT: applications in imaging technologies

# 4.1 Time-of-Flight Positron-Emission-Tomography

Time-of-Flight positron emission tomography (TOF PET) is a powerful technique used in medicine and medical research to image molecular processes in vivo. The best modern commercial systems can provide a coincidence time resolution (CTR) of about 210 ps [30], but the breakthrough in performance is expected when a CTR of 10 ps is achieved [31]. This will increase effective PET

sensitivity, as compared to the current state-of-the-art, at least a factor of 16, with the following expected consequences:

- Reduction of the radiation doses of molecular imaging procedures to negligibly low levels;
- Reduction of the synthesized quantity of radiopharmaceutical needed for each examination, and thus of the relatively high cost currently associated with in-vivo molecular imaging procedures;
- Further extension of the benefit of molecular imaging procedures beyond oncology towards cardiovascular, neurological, metabolic, inflammatory, infectious or metabolic disease (such as diabetes), especially in the pediatric, neonatal, and prenatal contexts;
- Maximizing the spatial and temporal resolution of PET based molecular imaging;
- Providing precise dynamic studies of molecular processes of high interest in pharmacology for screening and selecting candidate molecules for the next generation of drugs or new applications thereof;
- Potentially providing further extension of molecular in-vivo imaging to study "systems biology" of the whole human body through whole-body imaging systems;
- Eliminating the need for full angular coverage of the patient, opening many new opportunities for PET system design.

The RFPMT is an excellent candidate to achieve such performance when combined with a Cherenkov radiator such as crystalline PbF<sub>2</sub> [32, 33] or TMBi liquid [34]. High resolution could also be achieved by using fast scintillator and an RFPMT with a spiral scanning system and pixelated anode [35].

### 4.2 Time-of-Flight Diffuse-Optical-Tomography

Optical techniques have particular therapeutic potential in the medical field, because visible and infrared (IR) light is, unlike x rays, non-ionizing. Moreover, different types of tissues interact differently with visible light. One of the most useful features is the difference in the absorption coefficient at 700 nm of oxidized and non-oxidized hemoglobin, which can be utilized not only in identifying an activated metabolism but also in tumor detection [36, 37]. In addition, the scattering coefficient depends sensitively on the cells' organelles, such as the nucleus and mitochondria. Therefore, visible, and near-IR light is extremely useful for diagnosing different anomalies in biological tissue. Optical imaging in general and optical mammography are therefore among the holy grails of clinical imaging [38]. It has recently been shown that spatially resolved TOF information of the photons transmitted through semi-opaque tissue, analyzed with an advanced computational imaging technique, can detect hidden objects at cm depths with a resolution of a few mm. This can be improved by increasing both the spatial and temporal resolution of the detected photons [39, 40]. Time Correlated Single Photon Counting (TCSPC), employing multiple RFPMTs to detect the scattered photons at different positions and angles, then gives measurements of the time distributions of photons after they leave the sample via different propagation paths.

# 5 Summary

The new RF Timing technique, capable of providing picosecond resolution at MHz counting rates, is described. It is based on a helical deflector, which performs circular or elliptical sweeps of keV electrons by means of a radio frequency electromagnetic field lying in the 500–1000 MHz range. By converting the time of arrival of incident electrons to a hit position on a circle or ellipse, the RF Timer has demonstrated a timing resolution of 10 ps. This is mainly due to the technical parameters of the prototype tube and can certainly be improved. The RF Timer based single photon and fission fragment detectors are planned to be employed in nuclear studies as well as in imaging technologies. Applications in hypernuclear and shape isomer studies, as well as in TOF-PET, TOF-DOT are outlined.

# Acknowledgments

This work was partially supported by the Science Committee of the Republic of Armenia (Grants: 21T-2J133, 20TTCG-1C011 and 23LCG-1C018), UKRI STFC GRANT ST/V00106X/1 and the ARPA Institute.

#### References

- [1] A. Margaryan et al., An RF timer of electrons and photons with the potential to reach picosecond precision, Nucl. Instrum. Meth. A 1038 (2022) 166926.
- [2] A. Aprahamian et al., Advanced Radio Frequency Timing AppaRATus (ARARAT) Technique and Applications, arXiv:2211.16091.
- [3] B. Korzh et al., Demonstration of sub-3 ps temporal resolution with a superconducting nanowire single-photon detector, Nature Photon. 14 (2020) 250 [arXiv:1804.06839].
- [4] O. Jagutzki et al., *A position- and time-sensitive photon-counting detector with delay-line read-out, Proc. SPIE* **6585** (2007) 65851C [physics/0703186].
- [5] L. Gevorgian et al., A Radio Frequency Helical Deflector for keV Electrons, Nucl. Instrum. Meth. A 785 (2015) 175 [arXiv:1409.4593].
- [6] E. Delagnes, D. Breton, H. Grabas, J. Maalmi, P. Rusquart and M. Saimpert, *The SAMPIC Waveform and Time to Digital Converter*, in the proceedings of the 2014 IEEE Nuclear Science Symposium and Medical Imaging Conference (NSS/MIC), Seattle, WA, U.S.A. (2014), p. 1–9 [DOI:10.1109/NSSMIC.2014.7431231].
- [7] https://www.picotech.com/products/oscilloscope.
- [8] A. Margaryan et al., Radio frequency picosecond phototube, Nucl. Instrum. Meth. A 566 (2006) 321.
- [9] V. Tsakanov, *Test Facility for Advanced Accelerator and Radiation Sources Concepts*, http://candle.am/wp-content/uploads/2015/10/V-Tsakanov-AREAL-Part1.pdf (2015).
- [10] A. Margaryan et al., Single Photon THz Timer, Armenian J. Phys. 10 (2017) 23.
- [11] X. Llopart et al., Timepix4, a large area pixel detector readout chip which can be tiled on 4 sides providing sub-200 ps timestamp binning, 2022 JINST 17 C01044.
- [12] H. Nemura, Y. Akaishi and Y. Suzuki, *Ab initio Approach to s-Shell Hypernuclei*  $^3_{\Lambda}$ H,  $^4_{\Lambda}$ H,  $^4_{\Lambda}$ He, and  $^5_{\Lambda}$ He with a  $\Lambda N \Sigma N$  Interaction, *Phys. Rev. Lett.* **89** (2002) 142504 [nucl-th/0203013].

- [13] A. Gal, Charge symmetry breaking in  $\Lambda$  hypernuclei revisited, Phys. Lett. B **744** (2015) 352 [arXiv:1503.01687].
- [14] D. Gazda and A. Gal, *Ab initio Calculations of Charge Symmetry Breaking in the A* = 4 *Hypernuclei*, *Phys. Rev. Lett.* **116** (2016) 122501 [arXiv:1512.01049].
- [15] A. Margaryan, O. Hashimoto, S. Majewski and L. Tang, *Study of Hypernuclei by Pionic Decay*, Letter of Intent LOI-07-001, Jefferson Lab (2006).
- [16] A. Margaryan et al., *Study of Light Hypernuclei by Pionic Decay at JLab*, Experimental Proposal E-08-012, Jefferson Lab (2007).
- [17] A. Esser et al., Prospects for hypernuclear physics at Mainz: From KAOS@MAMI to PANDA@FAIR, Nucl. Phys. A 914 (2013) 519.
- [18] A1 collaboration, Observation of  $^4_{\Lambda}H$  Hyperhydrogen by Decay-Pion Spectroscopy in Electron Scattering, *Phys. Rev. Lett.* **114** (2015) 232501 [arXiv:1501.06823].
- [19] A1 collaboration, Experimental investigations of the hypernucleus  $^4_{\Lambda}H$ , EPJ Web Conf. 113 (2016) 07001.
- [20] P. Achenbach et al., Strange hadrons strangeness in strongly interacting particles. Strangeness production with KAOS at MAMI, Eur. Phys. J. ST 198 (2011) 307.
- [21] A. Margaryan et al., High Precision Momentum Calibration of the Magnetic Spectrometers at MAMI for Hypernuclear Binding Energy Determination, Nucl. Instrum. Meth. A 846 (2017) 98 [arXiv:1608.01126].
- [22] A. Margaryan et al., Delayed Pion Spectroscopy of Hypernuclei, J. Phys. Conf. Ser. 496 (2014) 012006.
- [23] A. Margaryan et al., Tagged-weak pi method, Phys. Atom. Nucl. 74 (2011) 216.
- [24] A. Gal, E.V. Hungerford and D.J. Millener, *Strangeness in nuclear physics*, *Rev. Mod. Phys.* **88** (2016) 035004 [arXiv:1605.00557].
- [25] E. Botta, T. Bressani, S. Bufalino and A. Feliciello, Status and perspectives of experimental studies on hypernuclear weak decays, Riv. Nuovo Cim. 38 (2015) 387.
- [26] E. Bauer and G. Garbarino, On the role of ground state correlations in hypernuclear non-mesonic weak decay, Phys. Rev. C 81 (2010) 064315 [arXiv:0907.4199].
- [27] K. Itonaga and T. Motoba, Hypernuclear weak decays, Prog. Theor. Phys. Suppl. 185 (2010) 252.
- [28] HKS (JLAB E02-017) collaboration, *Direct measurements of the lifetime of medium-heavy hypernuclei*, *Nucl. Phys. A* **973** (2018) 116 [arXiv:1212.1133].
- [29] S. Garg et al., Atlas of nuclear isomers Second edition, Atom. Data Nucl. Data Tabl. 150 (2023) 101546 [arXiv:2208.01028].
- [30] J. van Sluis et al., Performance Characteristics of the Digital Biograph Vision PET/CT System, J. Nucl. Med. 60 (2019) 1031.
- [31] P. Lecoq et al., Roadmap toward the 10 ps time-of-flight PET challenge, Phys. Med. Biol. 65 (2020) 21RM01.
- [32] S. Korpar et al., Study of a Cherenkov TOF-PET module, Nucl. Instrum. Meth. A 732 (2013) 595.
- [33] C. Canot et al., Fast and Efficient Detection of 511 keV Photons using Cherenkov Light in PbF<sub>2</sub> Crystal coupled to a MCP-PMT and SAMPIC Digitization Module, 2019 JINST 14 1200 [arXiv:1909.06107].
- [34] D. Yvon et al., CaLIPSO: An novel detector concept for PET imaging, IEEE Trans. Nucl. Sci. 61 (2014) 60.
- [35] A. Margaryan, V. Kakoyan and S. Knyazyan, *Time-of-Flight positron emission tomography with radiofrequency phototube*, *Acta Phys. Polon. B Proc. Suppl.* **4** (2011) 107.

- [36] P. Vaupel, K. Schlenger, C. Knoop and M. Höckel, Oxygenation of human tumors: evaluation of tissue oxygen distribution in breast cancers by computerized O<sub>2</sub> tension measurements, Cancer Res. **51** (1991) 3316.
- [37] P. Vaupel, O. Thews, D.K. Kelleher and M. Hoeckel, *Current Status of Knowledge and Critical Issues in Tumor Oxygenation*, in *Oxygen Transport to Tissue XX*, A.G. Hudetz and D.F. Bruley eds., Springer US, Boston, MA, U.S.A. (1998), p. 591–602 [DOI:10.1007/978-1-4615-4863-8\_70].
- [38] B. Brezner et al., *Ballistic imaging of biological media with collimated illumination and focal plane detection*, *J. Biomed. Opt.* **20** (2015) 076006.
- [39] J. Radford, A. Lyons, F. Tonolini and D. Faccio, *Role of late photons in diffuse optical imaging*, *Opt. Express* **28** (2020) 29486.
- [40] Y. Zhao et al., High Resolution, Deep Imaging Using Confocal Time-of-flight Diffuse Optical Tomography, IEEE Trans. Pattern Anal. Machine Intell. 43 (2021) 2206.